Research Square

Preprints are preliminary reports that have not undergone peer review.
They should not be considered conclusive, used to inform clinical practice,
or referenced by the media as validated information.

Pancreatic functional damage and reversion to normoglycaemia after STZ-induced diabetes in minipigs: evidence of preserved coupling between [^{18}F]FDOPA PET and glucose regulation

Beatriz Perez-Guille
Instituto Nacional de Pediatría: Instituto Nacional de Pediatria
Ailema Gonzalez-Ortiz
Instituto Nacional de Pediatría: Instituto Nacional de Pediatria
Arturo Avendaño-Estrada
Universidad Nacional Autónoma de México: Universidad Nacional Autonoma de Mexico
Rosa Eugenia Soriano-Rosales
Instituto Nacional de Pediatría: Instituto Nacional de Pediatria
Leonardo Baruch Rios-Garcia
Instituto Nacional de Pediatría: Instituto Nacional de Pediatria
Carlos Cedillo-Pelaez
Instituto Nacional de Pediatría: Instituto Nacional de Pediatria
Jose Francisco Gonzalez-Zamora
Instituto Nacional de Pediatría: Instituto Nacional de Pediatria
Miguel Angel Avila-Rodriguez
Universidad Nacional Autónoma de México: Universidad Nacional Autonoma de Mexico
Rosa Maria Palma-Rosillo
Instituto Nacional de Pediatría: Instituto Nacional de Pediatria
Miguel Angel Olarte-Casas
Universidad Nacional Autónoma de México: Universidad Nacional Autonoma de Mexico
Claudia Contreras-Rivera
Universidad Nacional Autónoma de México: Universidad Nacional Autonoma de Mexico
MARIA ELENA TRUJILLO
elenam@unam.mx

Universidad Nacional Autonoma de Mexico https://orcid.org/0000-0002-7229-260X

Research Article

Keywords: Continuous glucose monitoring, [¹⁸F]FDOPA PET, Pancreatic function, Glycaemic variability, Reversion to normoglycaemia, Minipig model.

Posted Date: November 4th, 2026

DOI: https://doi.org/10.21203/rs.3.rs-11307602/v1

License: This work is licensed under a Creative Commons Attribution 4.0 International License.
Read Full License

Pancreatic functional damage and reversion to normoglycaemia after STZ-induced diabetes in minipigs: evidence of preserved coupling between [^{18}F]FDOPA PET and glucose regulation

Beatriz E Pérez-Guillé[1,2], Ailema González-Ortiz [1], Arturo Avendaño-Estrada[3,4], Rosa Eugenia Soriano-Rosales[1] Leonardo Baruch Ríos-García[1], Carlos Cedillo-Peláez[5], José Francisco González-Zamora[1], Miguel Ángel Ávila-Rodríguez[3,4], Rosa María Palma-Rosillo[6], Miguel Angel Olarte-Casas[7], Claudia Contreras-Rivera[7], María Elena Trujillo[2*]

1. Translational Research Center, Instituto Nacional de Pediatría, Mexico City, Mexico.

2. Facultad de Medicina Veterinaria y Zootecnia, Programa de Maestría y Doctorado en Ciencias de la Producción y Salud Animal. Universidad Nacional Autónoma de México, Mexico City, Mexico

3. Unidad de Radiofarmacia-Ciclotrón. Facultad de Medicina, División Investigación, Universidad Nacional Autónoma de México, Mexico City, Mexico.

4. Centro de Investigación sobre el Envejecimiento, CINVESTAV Sede Sur, Mexico City, Mexico

5. Experimental Immunology Laboratory, Instituto Nacional de Pediatría, Mexico City, Mexico.

6. Servicio de Medicina Nuclear, Instituto Nacional de Pediatría. Mexico City, Mexico

7. Unidad PET/CT Facultad de Medicina, Universidad Nacional Autónoma de México. Mexico City, Mexico

2.-*. Facultad de Medicina Veterinaria y Zootecnia, Universidad Nacional Autónoma de México, Mexico City, Mexico. Corresponding author: elenam@unam.mx

ORCID
Beatriz E Pérez-Guillé 0000-0001-7223-9449
Ailema Gonzalez-Ortiz 0000-0002-8891-9892
Arturo Avendaño-Estrada 0000-0002-7089-4797
Rosa E Soriano-Rosales 0000-0002-8966-8810
Leonardo B Rios-García 0009-0003-7101-360X
Carlos Cedillo-Pelaez 0000-0001-7899-6598
José F Gonzalez-Zamora 0000-0001-5444-270X
Miguel A Avila-Rodriguez 0000-0002-3060-410X
Rosa M Palma-Rosillo
Miguel A Olarte-Casas 0000-0002-8499-5644
Claudia Contreras-Rivera 0009-0008-7915-1499
María Elena Trujillo-Ortega 0000-0002-7229-260X

ABSTRACT

Purpose
To evaluate the relationship between pancreatic functional damage and reversion to normoglycaemia after streptozotocin (STZ)-induced diabetes in adult minipigs, and the associations of 6-[^{18}F]fluoro-L-3,4-dihydroxyphenylalanine ([^{18}F]FDOPA) uptake with insulin-positive area and glucose dynamics.
Methods
Twelve adult male minipigs (15–22 kg, 10 months old) with STZ-induced (150 mg/kg) pancreatic β-cell injury were followed for 30 days. Continuous glucose monitoring assessed interstitial glucose and glycaemic variability. Reversion was defined as fasting interstitial glucose at day 30 within the cohort baseline range (40–66 mg/dL). [^{18}F]FDOPA PET/CT was performed at baseline, day 15, and day 30 (±3 days). Pancreatic functional damage was estimated from changes in the pancreatic-to-splenic uptake ratio (SUVr), and insulin-positive area was quantified histologically.
Results
Three of 12 minipigs (25%) achieved reversion to normoglycaemia. At day 30, reversion animals had lower interstitial glucose (46.0 vs. 130.5 mg/dL, $p = 0.013$) and glycaemic variability (CV 15.5% vs. 23.7%, $p = 0.021$). Pancreatic tail SUVrmean was higher in the reversion group at day 15 (1.9 [1.4–1.9] vs. 1.3 [1.2–1.4], $p = 0.033$). Pancreatic head [^{18}F]FDOPA uptake correlated with insulin-positive area ($r \approx 0.74$, $p < 0.05$), whereas functional damage alone did not fully discriminate between groups.
Conclusion
Reversion to normoglycaemia after STZ-induced diabetes in minipigs represents a dynamic functional phenotype that is not solely explained by the magnitude of pancreatic injury. [^{18}F]FDOPA PET may reflect residual endocrine function and highlights a non-linear relationship between pancreatic damage and metabolic outcome.

RUNNING TITLE

[^{18}F]FDOPA PET and normoglycaemia reversion in diabetic minipigs

KEYWORDS

Continuous glucose monitoring; [^{18}F]FDOPA PET; Pancreatic function; Glycaemic variability; Reversion to normoglycaemia; Minipig model.

INTRODUCTION

Diabetes is a major and increasing global public health concern. According to the International Diabetes Federation (IDF, 2025), approximately one in nine adults lives with diabetes, underscoring the need for research into disease mechanisms and interventions that prevent progression and complications [1].

Animal models are central to translational diabetes research. Pigs are valuable biomedical models because their pancreatic physiology and glucose metabolism resemble those of humans [2, 3]. Minipigs are particularly suitable for studying type 1 diabetes mellitus (T1DM) and associated metabolic, functional, and histopathological changes [4, 5].

Streptozotocin (STZ), a cytotoxic agent with selective affinity for pancreatic β-cells, is widely used to induce experimental T1DM in minipigs and reliably produces hyperglycaemia and systemic diabetic alterations [2, 5]. Continuous glucose monitoring (CGM) has further improved

characterisation of the dynamic metabolic response to β-cell injury [6-8]. Importantly, some STZ-treated minipigs may show partial functional recovery. Niu et al. reported spontaneous normalisation of glycaemic parameters after the acute phase, suggesting compensatory mechanisms, β-cell regeneration, or preservation of residual endocrine function [8].

Accurate assessment of residual pancreatic endocrine function is therefore relevant when interpreting chemical ablation models. Dopamine receptors are expressed on β-cells, and dopamine is generated from L-DOPA through L-DOPA decarboxylase [9]. Accordingly, positron emission tomography (PET) using 6-[^{18}F]fluoro-L-DOPA ([^{18}F]FDOPA) has been explored for in vivo assessment of pancreatic endocrine function [10]. [^{18}F]FDOPA PET/CT is clinically established for localising focal lesions in congenital hyperinsulinism, where tracer accumulation identifies metabolically active pancreatic tissue [11, 12]. Alternative tracers targeting β-cell biomarkers, including the glucagon-like peptide-1 receptor, have also been investigated, although sensitivity to dynamic β-cell loss in large-animal models may be limited [13, 14].

However, the quantitative relationship between STZ-induced pancreatic functional damage and reversion to normoglycaemia remains poorly characterised in minipigs, particularly during the first four weeks after injury. Interindividual variation in STZ response and possible endocrine recovery further complicate the interpretation of these models.

The objective of this study was to evaluate the relationship between pancreatic functional damage and reversion to normoglycaemia four weeks after STZ-induced pancreatic β-cell injury in adult minipigs by integrating metabolic parameters, [^{18}F]FDOPA PET/CT, and histopathological findings.

MATERIALS AND METHODS

Study design and ethical approval

This preclinical study followed adult minipigs for 30 days after STZ-induced pancreatic β-cell injury. Procedures were approved by the Institutional Research Committee and Institutional Animal Care and Use Committee (IACUC-INP; INP 2021/026) and the UNAM Subcomité Institucional para el Cuidado y Uso de Animales Experimentales (SICUAE; protocol SICUAE.DC-2023/2-4) and conducted in accordance with the Guide for the Care and Use of Laboratory Animals in an AAALAC-accredited facility.

Animals and housing conditions

Thirteen male minipigs (*Sus scrofa domesticus*; 15–22 kg; 10 months old) were acclimatised for one month. Housing conditions complied with NOM-062-ZOO-1999 and international standards. Animals were housed individually under controlled environmental conditions (22–26°C; relative humidity 50% ± 20%), provided enrichment and daily socialisation, and monitored twice daily. A commercial minipig diet (Purina®, Jamonina) was provided at 1.5% body weight/day in two meals (09:00 and 17:00), with water ad libitum.

Induction of pancreatic β-cell damage with streptozotocin

After a 12-h fast, animals received 0.9% saline (10 mL/kg/h for 1 h); analgesia consisted of flunixin meglumine (2.2 mg/kg IV) and buprenorphine (0.1 mg/kg). General anaesthesia was induced intramuscularly with ketamine (2.2 mg/kg; Anesket®, Pisa, Mexico), xylazine (2.2 mg/kg; Rompun®, Bayer, Germany), tiletamine/zolazepam (4.4 mg/kg; Zoletil®, Virbac, Mexico), and atropine (0.05 mg/kg; Atropisa®, Pisa, Mexico). STZ (150 mg/kg) in citrate buffer (pH 4.5) was administered as a single intravenous bolus over 1 min [3].

Metabolic monitoring and glycaemic management

Blood glucose and liver and renal function tests were assessed at baseline and days 15 and 30. CGM was performed with a transdermal sensor in the biceps femoris region as previously described [6], recording interstitial glucose every 5 min. Baseline fasting values were defined from measurements between 00:00 and 08:00 h before STZ administration. Sustained fasting interstitial glucose ≥200 mg/dL prompted subcutaneous premixed insulin (70/30, intermediate/rapid-acting; 0.1–0.2 U/kg/day), adjusted according to clinical and glycaemic response. The experimental workflow is summarised in Figure 1.

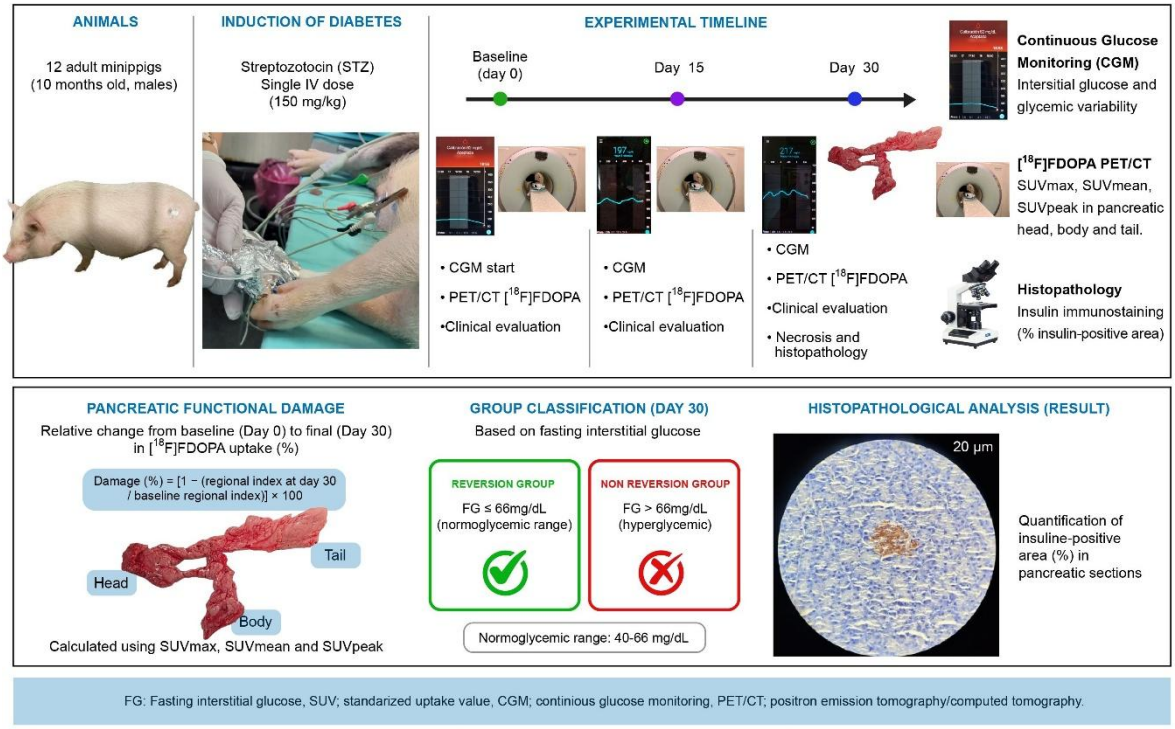


Fig. 1 Experimental design and multimodal assessment of pancreatic functional damage and glucose reversion in STZ-induced diabetic minipigs

Definition of reversion and non-reversion groups

Baseline fasting interstitial glucose values across all animals were used to define a study-specific normoglycaemic reference range of 40–66 mg/dL (mean, 53 mg/dL; SD, 13 mg/dL).

Animals with fasting interstitial glucose values within this range at day 30 were classified into the reversion group, whereas those with values above the range were classified into the non-reversion group.

Glycaemic variability was quantified as:

CV (%) = (SD / mean glucose) × 100

[^{18}F]FDOPA PET/CT imaging

PET/CT imaging was performed at baseline, 15 ± 2 days, and 30 ± 3 days after STZ administration. All scans were performed under general anaesthesia using the previously described anaesthetic protocol, with intravenous tiletamine/zolazepam supplementation as required. Heart rate and oxygen saturation (SpO_2) were monitored continuously throughout image acquisition using a tail-mounted monitoring device. [^{18}F]FDOPA (approximately 4.4 MBq/kg IV) was administered 60 min before imaging. Scans were acquired on a Siemens BIOGRAPH 6 PET/CT system using seven whole-body bed positions from head to feet (3 min/bed), followed by a dedicated abdominal acquisition centered on the pancreas. CT images were used for anatomical localisation and attenuation correction.

PET/CT image analysis

PET/CT images were analysed using syngo via software (Siemens Healthineers, Erlangen, Germany) with the Molecular Imaging application. Isocontour regions of interest (ROIs) were manually delineated on fused PET/CT images in the pancreatic head, body, and tail using CT anatomical guidance, avoiding adjacent structures and minimising partial-volume effects.

SUVmean, SUVmax, and SUVpeak were recorded for each ROI. A circular splenic reference ROI was used to calculate the pancreatic-to-splenic uptake ratio (SUVr):

SUVr = pancreatic SUV / splenic SUV

The spleen was selected rather than the liver because of the physiological involvement of the liver in peripheral [^{18}F]FDOPA metabolism. The resulting dimensionless SUVr was used for longitudinal comparisons and for calculation of pancreatic functional damage and late functional change.

Pancreatic functional damage

Pancreatic functional damage and late functional change were assessed longitudinally using SUVr, with each animal serving as its own reference.

Baseline-to-final pancreatic functional damage

Baseline-to-final pancreatic functional damage was calculated separately for each pancreatic region as:

Pancreatic functional damage (%) = [1 − (SUVr at final / SUVr at baseline)] × 100

This study-specific metric quantified the relative reduction in pancreatic [^{18}F]FDOPA uptake from baseline to day 30. Positive values indicated a decrease in SUVr relative to baseline. Negative values, corresponding to an increase in SUVr at day 30 relative to baseline, were assigned a value of 0%, because this metric was specifically intended to quantify functional loss rather than increases in tracer uptake**.**

Late functional change (day 15 to day 30)

Late functional change between the intermediate and final scans was calculated as:

Late functional change (%) = [1 − (SUVr at final / SUVr at intermediate)] × 100

This study-specific metric quantified the relative reduction in pancreatic [^{18}F]FDOPA uptake between day 15 and day 30. Positive values indicated a decrease in SUVr during this interval. Negative values, corresponding to an increase in SUVr from day 15 to day 30, were assigned 0% because the metric was intended to quantify reductions in tracer uptake rather than increases.

Pancreatic tissue collection and histological processing

At day 30, animals were euthanised by intravenous administration of pentobarbital (150 mg/kg) in accordance with the American Veterinary Medical Association (AVMA) Guidelines [15]. Post-mortem examination was performed in accordance with previously described veterinary pathology procedures [16, 17]. The entire pancreas was collected and divided into head, body, and tail regions.

Tissue samples were fixed in 10% neutral buffered formalin (pH 7.2) for 24 h, routinely processed, paraffin embedded, sectioned at 3–5 μm, and stained with haematoxylin and eosin (H&E). We obtained two representative sections from each pancreatic region for analysis.

Immunohistochemistry

Additional sections were immunostained for insulin using a rabbit polyclonal anti-insulin antibody (ab63820, Abcam; 1:1000) for 24 h, followed by a biotinylated secondary antibody (Thermo Scientific) and a streptavidin–biotin peroxidase detection method. Immunoreactivity was visualised using 3,3′-diaminobenzidine (DAB; Betazoid-DAB, Biocare) and counterstained with haematoxylin.

Digital image analysis

Immunostained slides were digitised at 40× magnification using the Aperio CS2 (Leica Biosystems) and analysed using QuPath software. Pancreatic tissue regions were manually annotated, excluding artefacts and non-representative areas. After colour deconvolution to separate haematoxylin and DAB signals, supervised pixel classification was used to quantify insulin-positive staining.

Histological assessment of the insulin-positive area

The primary histological outcome was the percentage of insulin-positive area relative to total pancreatic tissue area, calculated as:

Insulin-positive area (%) = (DAB-positive area / total pancreatic area) × 100

For each pancreatic region, the mean of two analysed sections was used for statistical analysis.

Statistical analysis

Continuous variables were assessed for normality using the Shapiro–Wilk test and summarised as medians and interquartile ranges (IQRs). Reversion and non-reversion groups were compared using the Mann–Whitney *U* test.

Pearson correlation analyses were performed to evaluate associations between interstitial glucose and pancreatic functional damage, and between PET-derived parameters and insulin-positive area.

Statistical analyses were performed using Stata version 16.1 (StataCorp LLC, College Station, TX, USA). Graphical representations were generated using GraphPad Prism (GraphPad Software, Boston, MA, USA). A p value < 0.05 was considered statistically significant.

RESULTS

Thirteen minipigs entered the study; 12 completed follow-up and were analysed. One animal died approximately 14 h after STZ administration from severe hypoglycaemia and was excluded.

Comparison of glycaemic parameters between reversion and non-reversion groups

Glycaemic parameters are shown in Figure 2. No significant baseline differences were observed between the reversion and non-reversion groups in blood glucose, interstitial glucose, or glycaemic variability.

At day 15, animals in the reversion group had significantly lower blood glucose concentrations than those in the non-reversion group (146.0 [133.0–191.0] vs. 335.7 [236.3–388.2] mg/dL, p = 0.033). Interstitial glucose was also lower, although the difference did not reach statistical significance (53.9 [47.9–127.3] vs. 183.6 [122.6–219.5] mg/dL, p = 0.052). Glycaemic variability was significantly lower in the reversion group (CV, 9.9% [9.6–16.4] vs. 21.2% [18.7–25.4], p = 0.033).

At day 30, animals in the reversion group had significantly lower blood glucose (97.0 [94.0–98.0] vs. 217.4 [199.4–310.9] mg/dL, p = 0.013), interstitial glucose (46.0 [42.4–60.0] vs. 130.5 [100.8–161.2] mg/dL, p = 0.013), and glycaemic variability (CV, 15.5% [14.0–17.6] vs. 23.7% [21.6–37.9], p = 0.021).

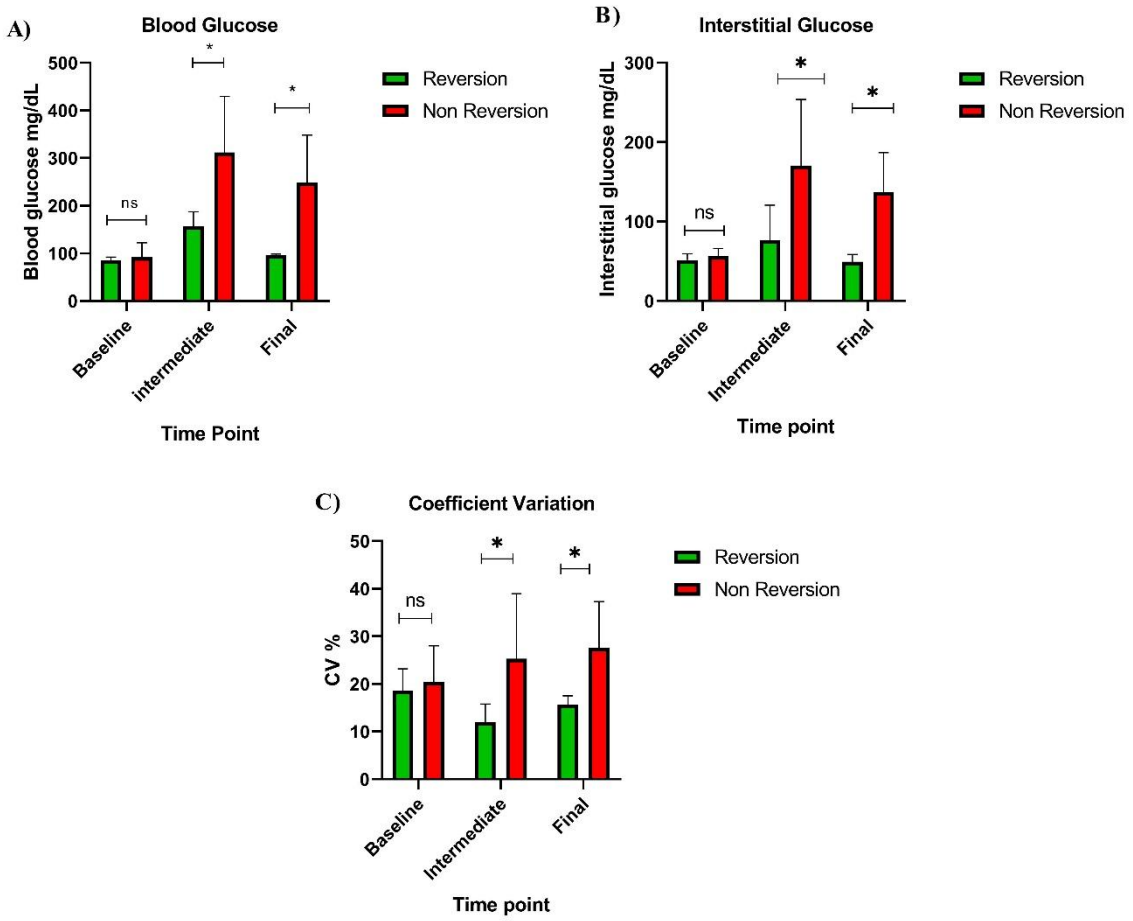


Fig. 2 Glycaemic parameters. (A) Blood glucose concentration, (B) interstitial glucose concentration, and (C) coefficient of variation (CV) of interstitial glucose in the reversion (n = 3) and non-reversion (n = 9) groups at baseline, day 15, and day 30. Data are presented as median (IQR). Group comparisons were performed using the Mann–Whitney *U* test. $p < 0.05$.

Descriptive and comparative analysis of [^{18}F]FDOPA uptake

Representative three-dimensional volume-rendered whole-body [^{18}F]FDOPA PET/CT images from the same minipig at baseline, day 15, and day 30 are shown in Figure 3, illustrating tracer biodistribution and prominent physiological accumulation in the urinary bladder.

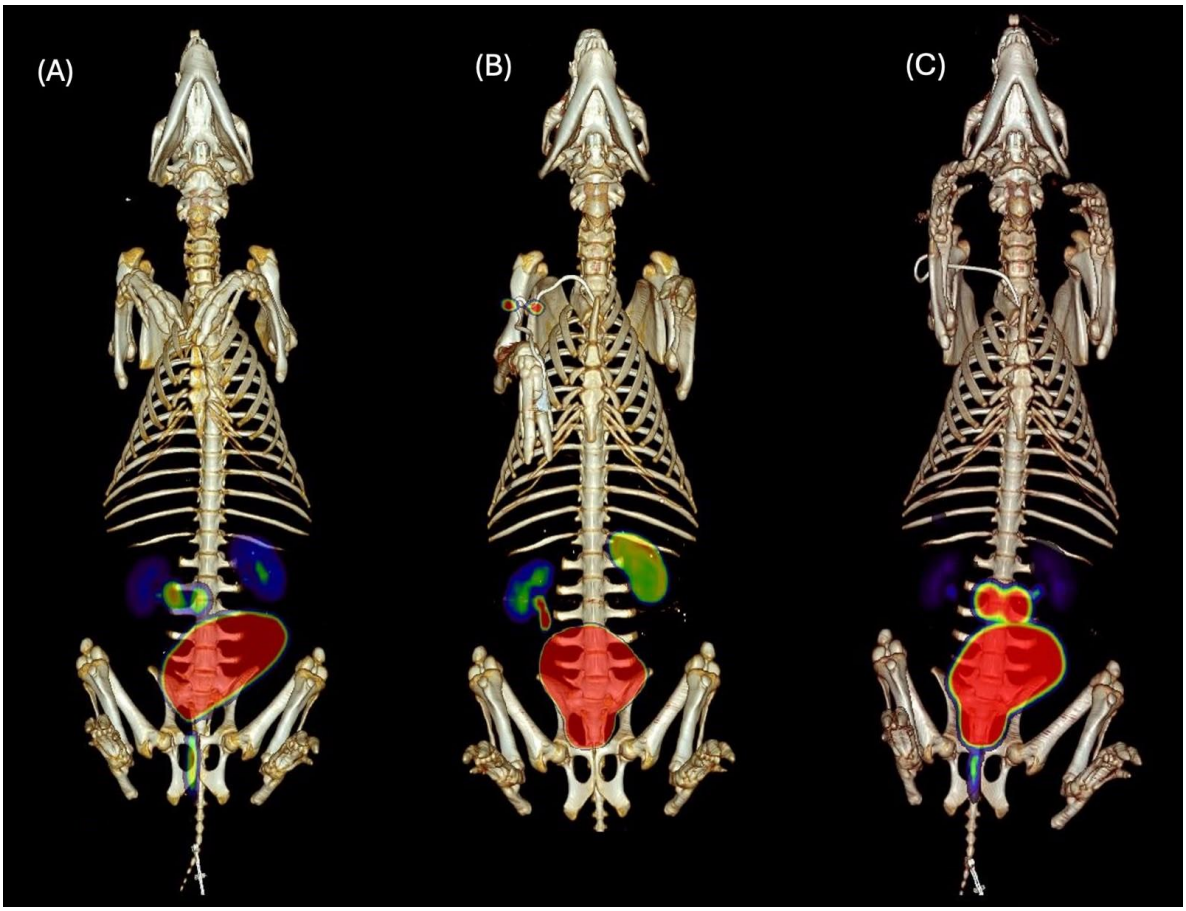


Fig. 3 Representative three-dimensional volume-rendered whole-body [^{18}F]FDOPA PET/CT images from the same minipig at baseline (A), day 15 ± 2 days (B), and day 30 ± 3 days (C), illustrating whole-body tracer biodistribution and prominent physiological accumulation in the urinary bladder.

Figure 4 shows pancreatic [^{18}F]FDOPA PET/CT images of the head, body, and tail in a representative non-reversion animal at baseline, day 15, and day 30, illustrating changes in tracer distribution and intensity following STZ administration.

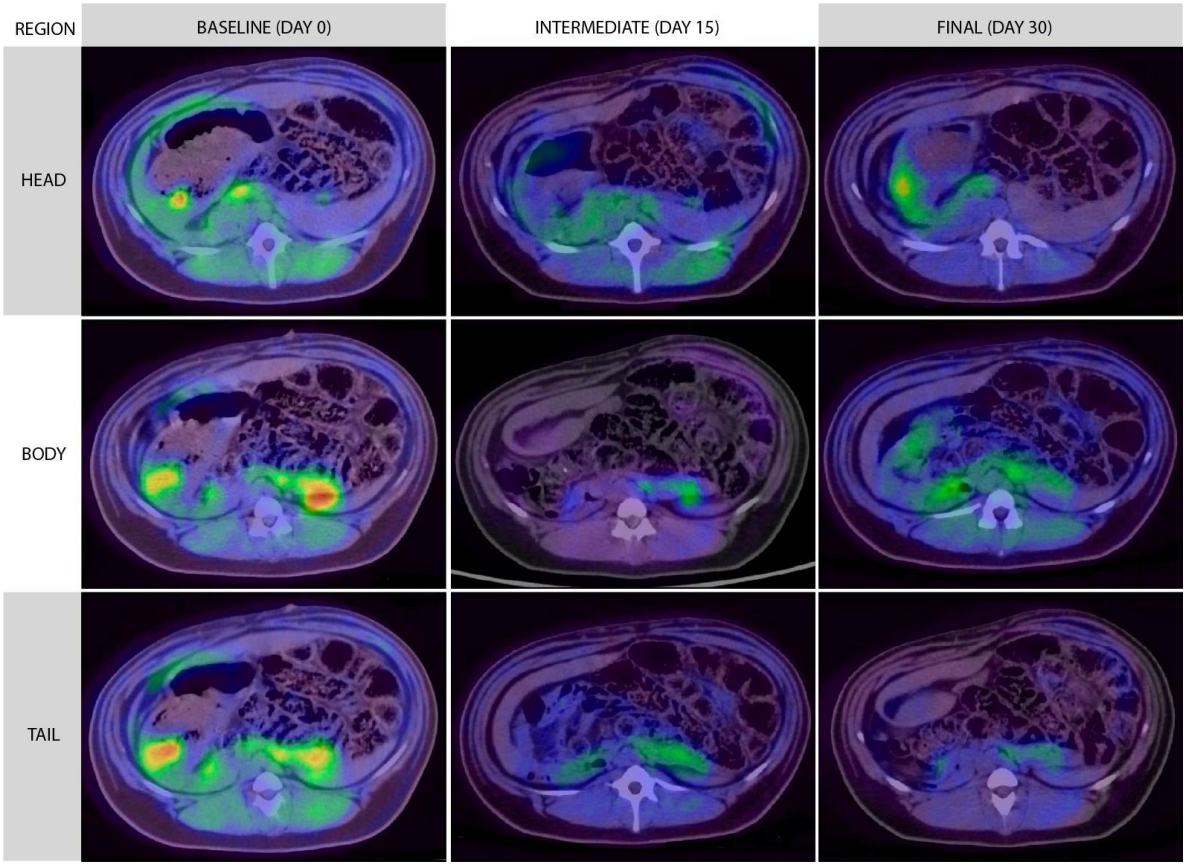


Fig. 4 Representative fused [^{18}F]FDOPA PET/CT images of the pancreatic head, body, and tail in a non-reversion minipig at baseline, day 15, and day 30, illustrating longitudinal changes in tracer uptake following STZ administration.

Pancreatic tail SUVrmean is compared between the reversion and non-reversion groups in Figure 5. Values did not differ significantly between groups at baseline ($p > 0.05$). On day 15, SUVmean was significantly higher in the reversion group (1.9 [1.4–1.9] vs. 1.3 [1.2–1.4], p = 0.033), whereas on day 30, the between-group difference was no longer significant ($p > 0.05$). Complete regional SUVrmean, SUVrmax, SUVrpeak, and body-weight data are provided in Supplementary Table S1.

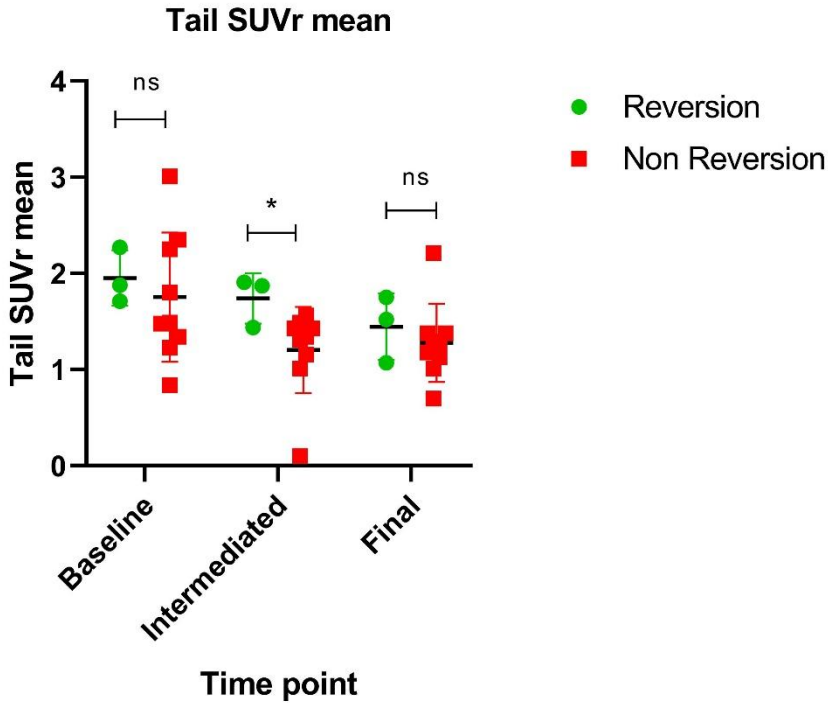


Fig. 5 Pancreatic tail SUVrmean in the reversion and non-reversion groups at baseline, day 15, and day 30. Data are presented as median (IQR). Group comparisons were performed using the Mann–Whitney *U* test. $p < 0.05$.

Individual metabolic and imaging profiles

Individual trajectories of blood glucose, interstitial glucose, and pancreatic tail SUVrmean are shown in Figure 6. Non-reversion animals generally exhibited higher glucose concentrations at later time points together with lower pancreatic [^{18}F]FDOPA uptake, whereas reversion animals showed more stable glycaemic profiles and relatively preserved or increased uptake.

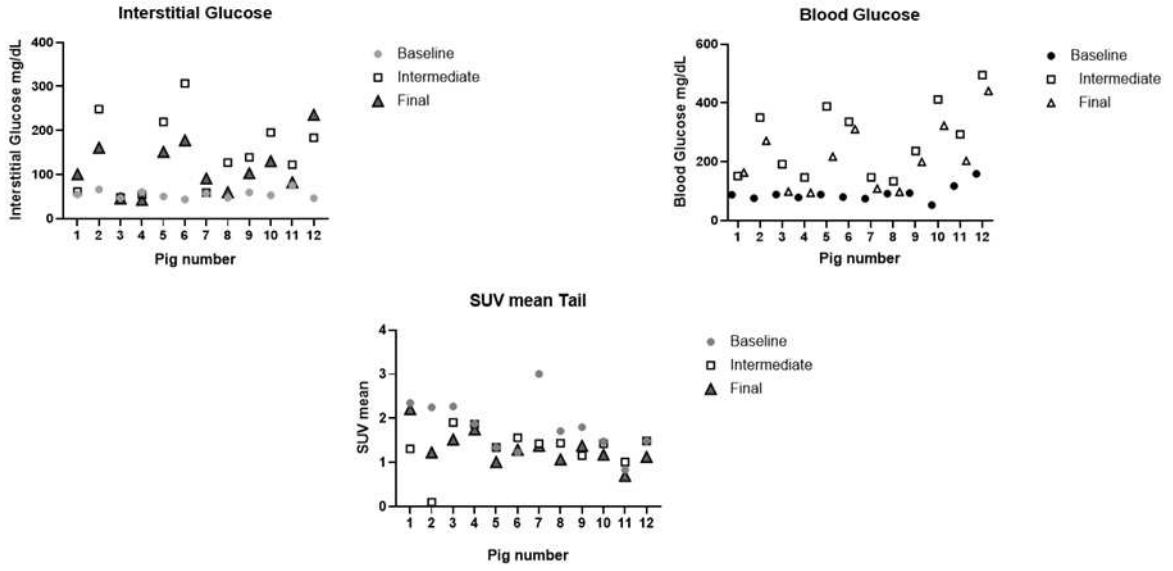


Fig. 6 Individual longitudinal profiles of blood glucose, interstitial glucose, and pancreatic tail [^{18}F]FDOPA SUVrmean at baseline, day 15 ± 2 days, and day 30 ± 3 days. Symbols indicate individual measurements for each minipig at the corresponding study time point.

Association between pancreatic [^{18}F]FDOPA uptake and final interstitial glucose

Within the reversion group (n=3), final interstitial glucose showed strong inverse correlations with pancreatic tail [^{18}F]FDOPA uptake, reaching statistical significance for SUVrpeak ($r=-0.998$, $p=0.039$) and SUVrmax ($r=-0.999$, $p=0.022$).

Baseline-to-final pancreatic functional damage

Baseline-to-final pancreatic functional damage derived from SUVrmean varied across animals and pancreatic regions (Figure 7). The pancreatic body showed the most consistent positive damage values, whereas the head and tail exhibited greater heterogeneity. Several animals had 0% values, indicating no measurable reduction in SUVr relative to baseline. Individual values are provided in Supplementary Table S2.

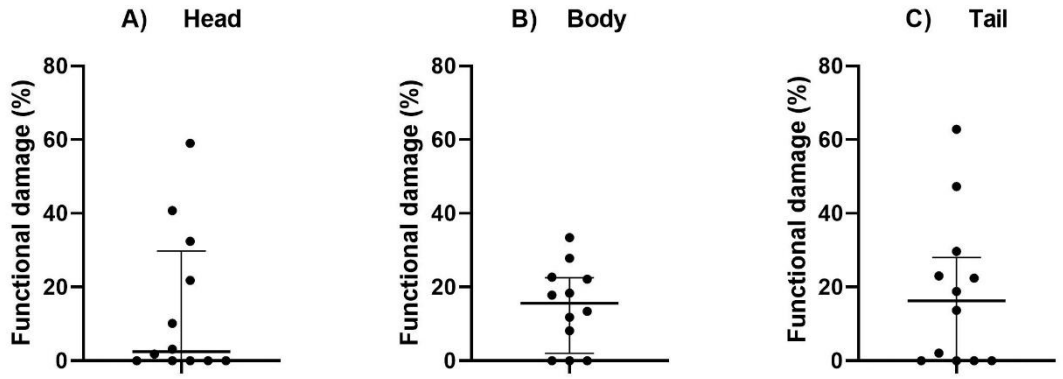


Fig. 7 Baseline-to-final pancreatic functional damage derived from SUVrmean in the pancreatic head (A), body (B), and tail (C). Each point represents an individual minipig; horizontal lines indicate the median and interquartile range (IQR).

Late functional change in pancreatic uptake (day 15 to day 30)

Late functional change in pancreatic [^{18}F]FDOPA uptake between day 15 and day 30 was heterogeneous across animals and pancreatic regions, with the largest reductions observed in the pancreatic tail (Supplementary Table S3). Several animals had values of 0%, indicating no measurable reduction in SUVr during this interval.

Histological findings and correlations with PET parameters

Representative insulin immunohistochemistry from the pancreatic head, body, and tail is shown in Figure 8. Reversion animals exhibited more extensive insulin-positive staining, whereas non-reversion animals showed reduced insulin immunoreactivity.

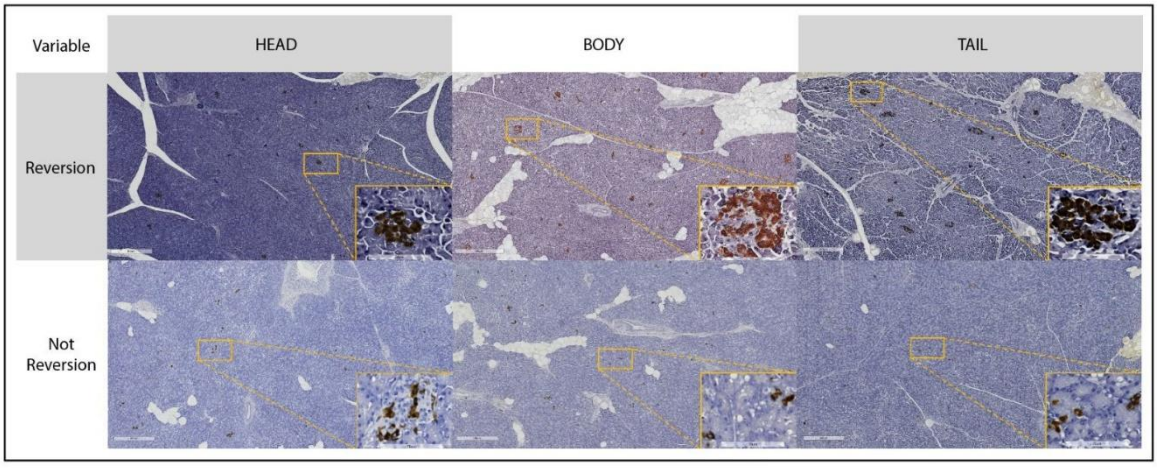


Fig. 8 Representative insulin immunohistochemistry in the pancreatic head, body, and tail from reversion and non-reversion minipigs. Insulin-positive cells are identified by brown DAB staining; insets show representative pancreatic islets from each region.

Correlation analyses were performed between PET-derived parameters and the percentage of insulin-positive area. At day 30, pancreatic head SUVrmean was positively correlated with insulin-positive area ($r = 0.74$, $p = 0.036$). Similarly, pancreatic head SUVrmax was positively correlated with insulin-positive area ($r = 0.73$, $p = 0.038$). The association between pancreatic head SUVrmean and insulin-positive area is shown in Figure 9.

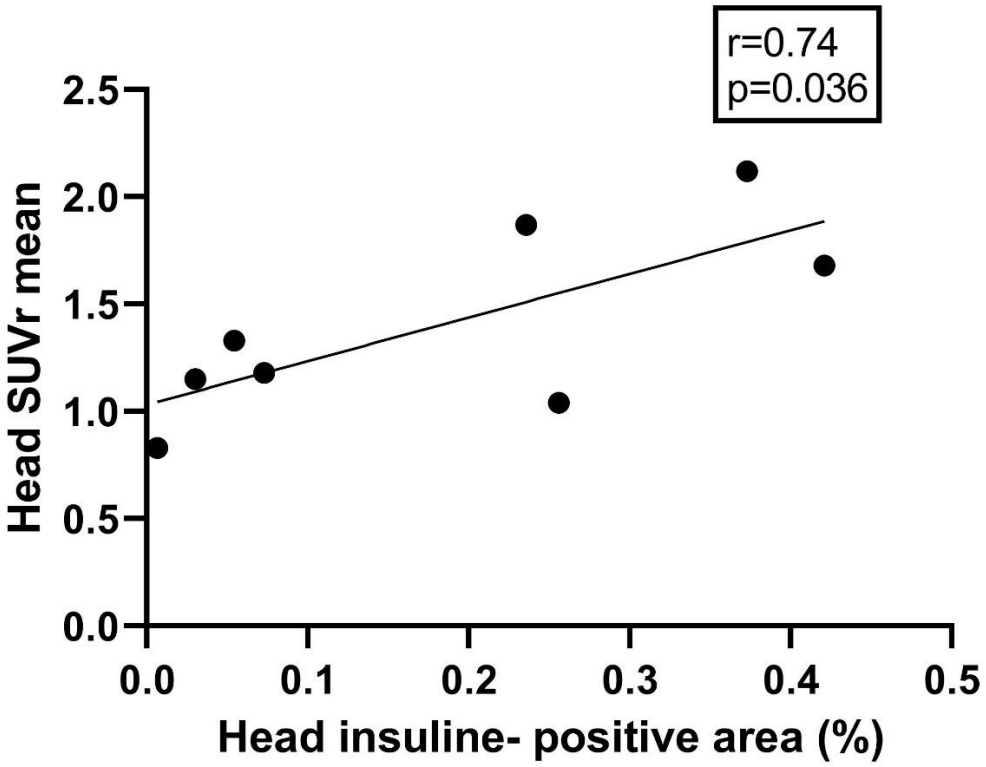


Fig. 9 Correlation between pancreatic head SUVrmean and insulin-positive area at day 30. Each point represents an individual minipig. The solid line indicates the linear regression fit. Pearson's $r = 0.74$, $p = 0.036$.

Pancreatic tail baseline-to-final functional change showed inverse, non-significant Pearson correlations with insulin-positive area for SUVrmean-derived change ($r = -0.74$, $p = 0.47$) and SUVrmax-derived change ($r = -0.85$, $p = 0.35$) among animals with available histological data (Figure 10).

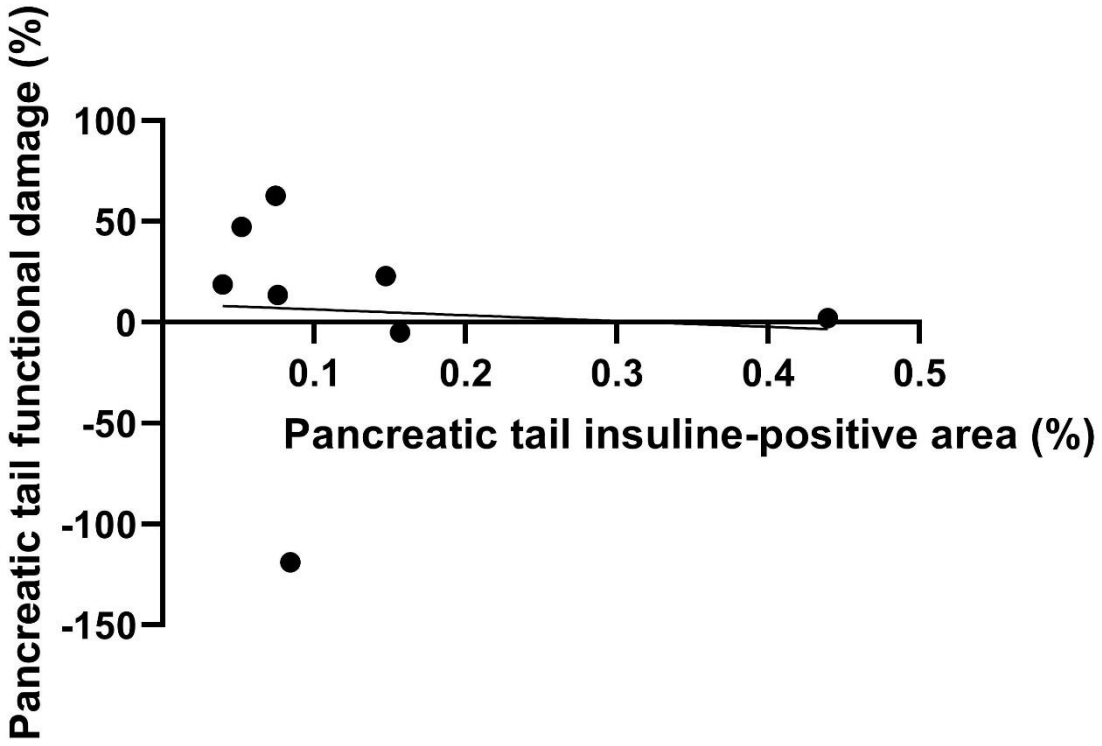


Fig. 10 Correlation between pancreatic tail functional damage and insulin-positive area in the reversion group. Negative trends were observed for SUVrmean-derived ($r = -0.74$, $p = 0.47$) and SUVrmax-derived damage ($r = -0.85$, $p = 0.35$)

DISCUSSION

This study demonstrates that reversion to normoglycaemia following STZ-induced diabetes in adult minipigs is characterised by distinct metabolic and histological patterns that can be captured using functional imaging. These findings support the concept that glycaemic reversion in this model is determined not solely by the magnitude of pancreatic injury but also by the preservation, adaptability, and residual functional capacity of surviving endocrine tissue.

A central observation was the clear metabolic distinction between reversion and non-reversion groups. Animals that returned to the predefined normoglycaemic range exhibited significantly lower interstitial glucose concentrations and reduced glycaemic variability at day 30. Notably, differences in glucose variability were evident as early as day 15, indicating that early glycaemic stabilisation may predict subsequent reversion. This observation is consistent with previous evidence suggesting that glycaemic variability is a sensitive marker of residual β-cell function and metabolic control, even in the absence of direct insulin measurements [6, 7]. In both experimental and clinical diabetes contexts, increased glucose variability has been associated with impaired endocrine reserve, oxidative stress, and adverse metabolic outcomes.

Spontaneous or delayed recovery following STZ-induced diabetes has also been reported in minipigs [8]. Niu et al. described a long-term Wuzhishan minipig model in which fasting glucose concentrations and intravenous glucose tolerance gradually normalised following STZ administration, suggesting the potential for β-cell functional recovery or endocrine compensation over time. Although the current study involved a shorter follow-up period, the observation that 25% of animals reverted to normoglycaemia by day 30 supports the notion that the diabetic phenotype in minipigs is dynamic rather than strictly irreversible. In long-term porcine models, persistent hyperglycaemia has been associated with diabetic nephropathy and retinal microvascular injury, further emphasising the translational relevance of this species for investigating both disease progression and metabolic recovery [8].

The minipig model is particularly advantageous for this type of research because of the significant anatomical and metabolic similarities between pigs and humans [2, 3, 5]. These features enhance the model's value in investigating the functional relationships among pancreatic injury, molecular imaging biomarkers, and glucose regulation. The larger body size of minipigs also facilitates repeated PET/CT imaging, CGM, and regional histological sampling, thereby increasing the translational relevance of this model compared with small-animal systems [18].

This study also provides new evidence regarding the behavior of [^{18}F]FDOPA PET in a large-animal translational model of pancreatic β-cell injury. At baseline, animals that subsequently achieved reversion generally exhibited higher pancreatic tracer uptake, suggesting that pre-existing endocrine functional reserve may influence the response to STZ. Although these baseline differences did not reach statistical significance, the observed trend is biologically plausible and consistent with previous studies demonstrating substantial interindividual variability in STZ sensitivity among pigs [3, 4]. Larsen et al. reported that, even within the same strain, glycaemic response to STZ varied considerably depending on baseline physiology, age, and β-cell reserve [3, 4].

At the intermediate time point, the reversion group exhibited significantly higher pancreatic tail SUVrmean. This regional observation is noteworthy because the pancreatic tail contains a relatively higher concentration of endocrine tissue in several mammalian species, including pigs, and may therefore more accurately reflect residual islet viability. Preservation of tracer uptake in this region may indicate maintained endocrine activity sufficient to support subsequent glucose normalisation.

A particularly important finding was the significant positive correlation between final pancreatic head [^{18}F]FDOPA uptake and the percentage of insulin-positive area. Both SUVrmean and SUVrmax correlated positively with histological insulin staining, supporting the hypothesis that [^{18}F]FDOPA uptake reflects viable endocrine activity rather than simply anatomical tissue volume. This interpretation aligns with the established clinical use of [^{18}F]FDOPA PET in congenital hyperinsulinism, in which tracer accumulation identifies metabolically active β-cell lesions [10, 12]. More broadly, molecular imaging studies increasingly recognise that PET biomarkers may indicate functional endocrine competence rather than absolute β-cell mass alone [13].

Previous research has emphasised the need for caution when interpreting pancreatic PET tracers in pigs. Nalin et al. reported that pancreatic uptake of the GLP-1 receptor radiotracer [^{68}Ga]Ga-DO3A-VS-Cys40-Exendin-4 was not reduced following STZ-induced β-cell destruction, indicating that some β-cell–targeted tracers may not perform in large-animal models as anticipated based on rodent studies [19]. In contrast, the present study demonstrated biologically meaningful associations between [^{18}F]FDOPA uptake, glycaemic phenotype, and insulin-positive area, supporting a cautious yet valuable interpretation of this tracer as a marker of residual endocrine functional activity.

The association between structural damage and metabolic outcome proved to be more complex than initially anticipated. In certain pancreatic regions, animals in the reversion group exhibited greater baseline-to-final reductions in normalised [^{18}F]FDOPA uptake than those in non-reversion animals. Although this observation may appear paradoxical, tracer reduction should not be regarded as a straightforward linear indicator of irreversible β-cell loss.

Consistent with these observations, the relationship between pancreatic functional damage and glucose reversion was not strictly linear. Although pancreatic functional damage quantified by [^{18}F]FDOPA PET reflected the extent of functional alteration, it did not fully distinguish between reversion and non-reversion groups. In some instances, animals that achieved reversion exhibited comparable or even greater reductions in tracer uptake than non-reversion animals. These results suggest that the magnitude of pancreatic injury alone is insufficient to predict metabolic outcome, and factors such as residual endocrine reserve, functional adaptation, and preserved pancreatic–glucose coupling are critical determinants of reversion.

A particularly notable finding was the strong positive correlation between pancreatic tail functional damage and interstitial glucose levels within the reversion group. In contrast, no significant association was detected in the non-reversion group. These results suggest that, in animals capable of reversion, glucose homeostasis remained physiologically linked to residual pancreatic function. Conversely, in non-reversion animals, this coupling appeared to be diminished, consistent with more advanced endocrine dysfunction and systemic dysregulation. Thus, surviving pancreatic tissue in reversion animals continued to exert a measurable metabolic influence, whereas in non-reversion animals this residual influence appeared to be insufficient.

The preserved association between pancreatic functional damage and interstitial glucose within the reversion group further suggests that glucose regulation remained coupled to residual pancreatic function. Reversion should therefore not be interpreted as absence of injury, but as preservation of sufficient endocrine reserve to maintain metabolic control. Dose-dependent and partially reversible diabetic phenotypes have previously been reported in porcine STZ models [3, 20]. Potential biological mechanisms include replication of surviving β-cells, endocrine-cell plasticity and transdifferentiation, neogenesis from progenitor populations, and microenvironmental support from endothelial and incretin signaling pathways [8, 21-34]. These mechanisms remain hypotheses in the present study because they were not directly measured.

In this context, the preserved coupling between [^{18}F]FDOPA uptake and glucose regulation observed in the reversion group may reflect both the presence of residual endocrine tissue and the functional maturation and integration of regenerated or adapted β-cells within the islet network. Since [^{18}F]FDOPA uptake is associated with amino acid metabolism and monoaminergic pathways involved in hormone processing, it may serve as a surrogate marker for both β-cell mass and functional activity [35-37]. Therefore, successful reversion likely requires not only structural recovery but also the restoration of coordinated insulin secretion and glucose responsiveness at the tissue level.

From a translational perspective, the integration of CGM, PET imaging, and histology constitutes a major strength of this study. CGM enabled dynamic metabolic phenotyping, PET/CT provided *in vivo* regional functional information, and histology offered endpoint structural confirmation. As no single modality fully captures the complexity of β-cell injury and recovery, their combined application provides a multidimensional approach that may be valuable for future studies evaluating regenerative therapies, islet transplantation, or β-cell preservation strategies.

Several limitations should be considered. The small number of animals achieving reversion reduced the precision of between-group comparisons and correlation analyses, although the observed reversion frequency itself represents a study outcome. Histological data were not available for all animals. In addition, [^{18}F]FDOPA is not β-cell-specific and its uptake may be influenced by amino acid transport, aromatic L-amino acid decarboxylase activity, inflammation, or regional perfusion.

CONCLUSION

Reversion to normoglycaemia after STZ-induced diabetes in adult minipigs was associated with lower interstitial glucose, reduced glycaemic variability, and preserved coupling between pancreatic activity and glucose regulation. [^{18}F]FDOPA PET was associated with glycaemic phenotype and insulin-positive pancreatic area, supporting its potential as an in vivo biomarker of residual endocrine function.

These findings indicate that reversion to normoglycaemia following STZ-induced diabetes should be regarded as a dynamic functional phenotype rather than merely a low-damage state. The integration of CGM, molecular imaging, and histopathology provides a robust multimodal framework for investigating pancreatic injury, functional recovery, and therapeutic response in translational diabetes research

ACKNOWLEDGMENTS

The authors express their gratitude to Sandra Iracema García Orozco, Sandra Galicia Pérez, Arturo Carmona Mancilla, Miranda Esquinca-Esquinca and Pedro Medina Granados for their assistance in developing this study, and to Juan Díaz Escorcia for his support in animal care, socialization, and treatment of the pigs involved in the research.

The authors also acknowledge the staff of the Nuclear Medicine Service at the Instituto Nacional de Pediatría (INP) for their invaluable collaboration in the execution of this project, especially the nuclear medicine technologists Julio César García Guzmán and Alberto Frías Bautista, as well as the MSc medical physicist Lorena López Beltrán and the radiochemist Ruth Santana Vázquez whose technical expertise and support were essential for the successful completion of the imaging studies.

References

1. Genitsaridi, I., et al., *11th edition of the IDF Diabetes Atlas: global, regional, and national diabetes prevalence estimates for 2024 and projections for 2050.* Lancet Diabetes Endocrinol, 2026. 14(2): p. 149-15610.1016/s2213-8587(25)00299-2.
2. Lunney, J.K., et al., *Importance of the pig as a human biomedical model.* Sci Transl Med, 2021. 13(621): p. eabd575810.1126/scitranslmed.abd5758.
3. Larsen, M.O. and B. Rolin, *Use of the Göttingen minipig as a model of diabetes, with special focus on type 1 diabetes research.* Ilar j, 2004. 45(3): p. 303-1310.1093/ilar.45.3.303.
4. Larsen, M.O., et al., *Mild streptozotocin diabetes in the Göttingen minipig. A novel model of moderate insulin deficiency and diabetes.* Am J Physiol Endocrinol Metab, 2002. 282(6): p. E1342-5110.1152/ajpendo.00564.2001.
5. Renner, S., et al., *Porcine models for studying complications and organ crosstalk in diabetes mellitus.* Cell Tissue Res, 2020. 380(2): p. 341-37810.1007/s00441-019-03158-9.

6. Pérez-Guillé, B.E., et al., *Description of Sensor Placement for Continuous Glucose Monitoring in a Pig Model of Diabetes Mellitus.* J Am Assoc Lab Anim Sci, 2025. 64(2): p. 310-610.30802/aalas-jaalas-24-096.
7. Izumi, M., et al., *Glucose and insulin responses following streptozotocin administration for the induction of a type 1 diabetes mellitus model in Microminipig.* J Vet Med Sci, 2025. 87(10): p. 1122-112710.1292/jvms.25-0145.
8. Niu, M., et al., *Long-term case study of a Wuzhishan miniature pig with diabetes.* Animal Model Exp Med, 2020. 3(1): p. 22-3110.1002/ame2.12098.
9. Rubí, B., et al., *Dopamine D2-like receptors are expressed in pancreatic beta cells and mediate inhibition of insulin secretion.* J Biol Chem, 2005. 280(44): p. 36824-3210.1074/jbc.M505560200.
10. Tinklepaugh, J. and N.E. Mamrak, *Imaging in Type 1 Diabetes, Current Perspectives and Directions.* Mol Imaging Biol, 2023. 25(6): p. 1142-114910.1007/s11307-023-01873-y.
11. Djekidel, M., *(18)F-FDOPA and (68)Ga-dotatate PET imaging in congenital hyperinsulinism.* Am J Nucl Med Mol Imaging, 2021. 11(3): p. 188-195,
12. Blomberg, B.A., et al., *The value of radiologic interventions and (18)F-DOPA PET in diagnosing and localizing focal congenital hyperinsulinism: systematic review and meta-analysis.* Mol Imaging Biol, 2013. 15(1): p. 97-10510.1007/s11307-012-0572-0.
13. Yang, J., et al., *Molecular imaging of diabetes and diabetic complications: Beyond pancreatic β-cell targeting.* Adv Drug Deliv Rev, 2019. 139: p. 32-5010.1016/j.addr.2018.11.007.
14. Eriksson, O., et al., *Glucagonlike Peptide-1 Receptor Imaging in Individuals with Type 2 Diabetes.* J Nucl Med, 2022. 63(5): p. 794-80010.2967/jnumed.121.262506.
15. Leary, S.L., et al., *AVMA Guidelines for the euthanasia of animals.* Animal Welfare, 2013,
16. de Aluja, A.S. and F.C. Casas, *Tecnicas de necropsia en animales domesticos*. 2002: Manual Moderno.https://books.google.com.bo/books?id=meTIAAAACAAJ
17. King, J., et al., *The necropsy book: a guide for veterinary students, residents, clinicians, pathologists, and biological researchers: Charles Louis Davis.* DVM Foundation, 2005,
18. Zhao, Y., et al., *Establishment of type 2 diabetes mellitus models using streptozotocin after 3 months high-fat diet in Bama minipigs.* Anim Biotechnol, 2023. 34(7): p. 2295-231210.1080/10495398.2022.2088548.
19. Nalin, L., et al., *Positron emission tomography imaging of the glucagon-like peptide-1 receptor in healthy and streptozotocin-induced diabetic pigs.* Eur J Nucl Med Mol Imaging, 2014. 41(9): p. 1800-1010.1007/s00259-014-2745-3.
20. Vériter, S., et al., *Improvement of pig islet function by in vivo pancreatic tissue remodeling: a "human-like" pig islet structure with streptozotocin treatment.* Cell Transplant, 2013. 22(11): p. 2161-7310.3727/096368912x657864.
21. Rankin, M.M. and J.A. Kushner, *Adaptive beta-cell proliferation is severely restricted with advanced age.* Diabetes, 2009. 58(6): p. 1365-7210.2337/db08-1198.
22. Demcollari, T.I., A.M. Cujba, and R. Sancho, *Phenotypic plasticity in the pancreas: new triggers, new players.* Curr Opin Cell Biol, 2017. 49: p. 38-4610.1016/j.ceb.2017.11.014.
23. Nir, T., D.A. Melton, and Y. Dor, *Recovery from diabetes in mice by beta cell regeneration.* J Clin Invest, 2007. 117(9): p. 2553-6110.1172/jci32959.
24. Chung, C.H., et al., *Pancreatic β-cell neogenesis by direct conversion from mature α-cells.* Stem Cells, 2010. 28(9): p. 1630-810.1002/stem.482.
25. Chakravarthy, H., et al., *Converting Adult Pancreatic Islet α Cells into β Cells by Targeting Both Dnmt1 and Arx.* Cell Metab, 2017. 25(3): p. 622-63410.1016/j.cmet.2017.01.009.
26. Chera, S., et al., *Diabetes recovery by age-dependent conversion of pancreatic δ-cells into insulin producers.* Nature, 2014. 514(7523): p. 503-710.1038/nature13633.

27. Xiao, X., et al., *Endogenous Reprogramming of Alpha Cells into Beta Cells, Induced by Viral Gene Therapy, Reverses Autoimmune Diabetes.* Cell Stem Cell, 2018. 22(1): p. 78-90.e410.1016/j.stem.2017.11.020.
28. Xu, X., et al., *Beta cells can be generated from endogenous progenitors in injured adult mouse pancreas.* Cell, 2008. 132(2): p. 197-20710.1016/j.cell.2007.12.015.
29. Gribben, C., et al., *Ductal Ngn3-expressing progenitors contribute to adult β cell neogenesis in the pancreas.* Cell Stem Cell, 2021. 28(11): p. 2000-2008.e410.1016/j.stem.2021.08.003.
30. Wang, D., et al., *Long-Term Expansion of Pancreatic Islet Organoids from Resident Procr(+) Progenitors.* Cell, 2020. 180(6): p. 1198-1211.e1910.1016/j.cell.2020.02.048.
31. Wang, J., et al., *Isolation of mouse pancreatic islet Procr(+) progenitors and long-term expansion of islet organoids in vitro.* Nat Protoc, 2022. 17(5): p. 1359-138410.1038/s41596-022-00683-w.
32. Cao, Z. and X. Wang, *The endocrine role between β cells and intra-islet endothelial cells.* Endocr J, 2014. 61(7): p. 647-5410.1507/endocrj.ej14-0045.
33. Wang, Y.J., et al., *Multiplexed In Situ Imaging Mass Cytometry Analysis of the Human Endocrine Pancreas and Immune System in Type 1 Diabetes.* Cell Metab, 2019. 29(3): p. 769-783.e410.1016/j.cmet.2019.01.003.
34. Chen, C., et al., *Human beta cell mass and function in diabetes: Recent advances in knowledge and technologies to understand disease pathogenesis.* Mol Metab, 2017. 6(9): p. 943-95710.1016/j.molmet.2017.06.019.
35. Eriksson, O., et al., *Positron Emission Tomography to Assess the Outcome of Intraportal Islet Transplantation.* Diabetes, 2016. 65(9): p. 2482-910.2337/db16-0222.
36. Eriksson, O., et al., *Positron emission tomography ligand [11C]5-hydroxy-tryptophan can be used as a surrogate marker for the human endocrine pancreas.* Diabetes, 2014. 63(10): p. 3428-3710.2337/db13-1877.
37. Adams, M.T. and B. Blum, *Determinants and dynamics of pancreatic islet architecture.* Islets, 2022. 14(1): p. 82-10010.1080/19382014.2022.2030649.

STATEMENTS AND DECLARATIONS

Funding

This work was funded by Project 2021/026, with support from the Q008 programme and resources provided by the Instituto Nacional de Pediatría. BP-G received a doctoral scholarship from the Secretaría de Ciencia, Humanidades, Tecnología e Innovación (SECIHTI; CVU 123171) as a student of the Programa de Maestría y Doctorado en Ciencias de la Producción y Salud Animal, Facultad de Medicina Veterinaria y Zootecnia, Universidad Nacional Autónoma de México. The study sponsor/funder was not involved in the design of the study; the collection, analysis and interpretation of data; writing the report; and did not impose any restrictions regarding publication of the report.

Competing interests

The authors have no relevant financial or non-financial interests to disclose.

Author contributions

All authors contributed to the study conception and design. Material preparation, data collection, and analysis were performed by Beatriz Pérez-Guillé, Ailema González-Ortiz, Arturo Avendaño-Estrada, María Elena Trujillo-Ortega, Rosa E Soriano-Rosales, Leonardo B Rios-Garcia, Jose F Gonzalez-Zamora, and Carlos Cedillo-Pelaez. Data processing and analysis. Miguel Angel Avila-Rodriguez, Rosa María Palma-Rosillo, Miguel Angel Olarte-Casas and Claudia Contreras-Rivera contributed to PET/CT acquisition, processing and image analysis. The first draft was written by Beatriz Pérez-Guillé, and all authors reviewed and approved the final manuscript.

Data availability

The datasets generated during and/or analysed during the current study are available from the corresponding author on reasonable request.

Ethics approval

All experimental procedures were approved by the Institutional Research Committee and the Institutional Animal Care and Use Committee (IACUC-INP) under registration number INP 2021/026 and the UNAM Subcomité Institucional para el Cuidado y Uso de Animales Experimentales (SICUAE; protocol SICUAE.DC-2023/2-4) and were conducted in accordance with the Guide for the Care and Use of Laboratory Animals.

Supplementary Files

This is a list of supplementary files associated with this preprint. Click to download.

- SUPPLEMENTARYINFORMATIONEJNMMIFINAL.pdf